*Acta metall. mater.* Vol. 41, No. 8, pp. 2365–2376, 1993
Printed in Great Britain. 

0956-7151/93 $6.00 + 0.00


# TRANSVERSE CRACKING IN FIBER-REINFORCED BRITTLE MATRIX, CROSS-PLY LAMINATES

**Z. C. XIA, R. R. CARR and J. W. HUTCHINSON**
Division of Applied Sciences, Harvard University, Cambridge, MA 02138, U.S.A.

*(Received 5 February 1993)*

**Abstract**—The topic addressed in this paper is transverse cracking in the matrix of the 90° layers of a cross-ply laminate loaded in tension. Several aspects of the problem are considered, including conditions for the onset of matrix cracking, the evolution of crack spacing, the compliance of the cracked laminate, and the overall strain contributed by release of residual stress when matrix cracking occurs. The heart of the analysis is the plane strain problem for a doubly periodic array of cracks in the 90° layers. A fairly complete solution to this problem is presented based on finite element calculations. In addition, a useful, accurate closed form representation is also included. This solution permits the estimation of compliance change and strain due to release of residual stress. It can also be used to predict the energy release rate of cracks tunneling through the matrix. In turn, this energy release rate can be used to predict both the onset of matrix cracking and the evolution of crack spacing in the 90° layers as a function of applied stress. All these results are used to construct overall stress–strain behavior of a laminate undergoing matrix cracking in the presence of initial residual stress.

## 1. INTRODUCTION

The macroscopic tensile properties of uni-directional fiber-reinforced brittle composites have been studied extensively since the 70's, where matrix cracking with intact fibers plays an important role in longitudinal strength. The transverse and shear strengths of such composites are invariably lower than the longitudinal strength. Consequently, in applications where multi-axial stress states are encountered, cross-ply laminates are commonly used. While there has been considerable attention to the elastic properties of cross-ply laminates, relatively less has been done to establish their fracture performance in terms of the properties of the constituent phases. This is the topic of the present paper where emphasis is on brittle matrix composites and explicit results for the effect of matrix cracking on overall stress–strain behavior are developed and presented. Studies of the topic have been carried out within a framework of damage mechanics where the effects of cracks are not explicitly predicted as represented by [1, 2]. More closely related to the present work are studies in [3, 4] where explicit results for the effect of cracks are given for general laminates. These four papers provide additional references to the general problem area.

Recently, a comprehensive experimental study was conducted on a laminated 0°/90° ceramic/matrix composite [5]. When the tensile stress was applied along one of the fiber directions, cracks were first observed in the 90° layer and always spanned the entire ply, but arrested at the interfaces between layers, as sketched in Fig. 1. With further increase of the applied stress, additional matrix cracks developed in the 90° layers in the same way as previous cracks. These cracks spread as 3D tunneling cracks from small flaws located on the matrix of the 90° layers in the direction transverse to the applied stress, as depicted in Fig. 1. At even higher applied stress, it was observed that the pre-existing cracks began to extend into the adjacent 0° layers stably and without any fiber failure, until these transverse cracks began overlapping in the 0° layers.

The work in this paper deals with conditions for the onset and subsequent multiplication of tunnel cracks in the 90° layers of cross-ply laminates. In addition, the effect of the tunnel cracks on the overall stress–strain relation of the composite will be determined, including the contribution from the release of residual stress. Such constitutive relations are required if progress is to be made in the effort to understand the role of micro-cracking in altering stress concentration at holes and notches in these materials. The paper is organized as follows. We begin by posing the problem for the energy release rate of steady-state tunnel cracks. This problem can be solved using information from a 2D plane strain problem, which also provides the results needed for the desired constitutive changes. Extensive finite element calculations are then reported, providing conditions for the onset of tunnel cracking and for subsequent multiple crack formation. The results permit one to predict the spacing expected between the 90° layer matrix cracks as a function of the applied stress. Given crack spacing in terms of applied stress, one can then predict the overall stress–strain behavior. This point is illustrated by giving examples of stress–strain behavior as a function of the basic geometry of the composite, the toughness of the matrix, and the residual stress in the

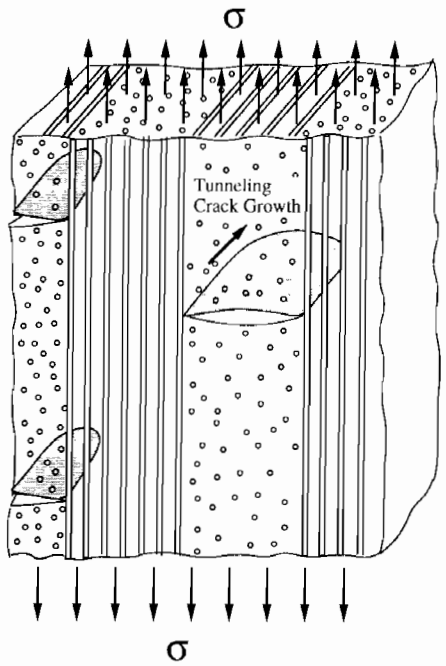


Fig. 1. A schematic of the 3D tunneling cracks in the 90° layers.

next section. An approximate analysis is carried out in the final section leading to closed form expressions for the overall compliance change and the tunneling energy release rate as a function of crack density. These results, which are quite accurate, will be very useful for practical applications.

## 2. BASIC MECHANICS

### *2.1. Basic equations for laminates*

The elastic properties of an undamaged unidirectional fiber reinforced ply are accurately taken to be transversely isotropic about the fiber direction. With the fibers aligned with the 1-axis, the constitutive relation for the undamaged ply is

$$\epsilon_{11} = \frac{1}{E_L}\sigma_{11} - \frac{\nu_L}{E_L}(\sigma_{22}+\sigma_{33})$$

$$\epsilon_{22} = -\frac{\nu_L}{E_L}\sigma_{11} + \frac{1}{E_T}\sigma_{22} - \frac{\nu_T}{E_T}\sigma_{33}$$

$$\epsilon_{33} = -\frac{\nu_L}{E_L}\sigma_{11} - \frac{\nu_T}{E_T}\sigma_{22} + \frac{1}{E_T}\sigma_{33}$$

$$\epsilon_{23} = \frac{1}{2\mu_L}\sigma_{23} \quad \epsilon_{13} = \frac{1}{2\mu_T}\sigma_{13} \quad \epsilon_{12} = \frac{1}{2\mu_T}\sigma_{12} \tag{1}$$

where the subscript L stands for longitudinal properties and the subscript T stands for transverse properties. Notice that $\mu_T = E_T/[2(1+\nu_T)]$ but generally $\mu_L \neq E_L/[2(1+\nu_L)]$.

To limit the number of material parameters in the subsequent development, the difference between the fiber and matrix Poisson's ratios will be neglected (i.e. $\nu_m = \nu_f = \nu$). This approximation is known to involve little error. The moduli of the ply are related to the constituent properties by

$$E_L = cE_f + (1-c)E_m \tag{2}$$

$$\mu_L = \frac{\mu_f(1-c)+\mu_m(1-c)}{\mu_f(1-c)+\mu_m(1+c)}\mu_m \tag{3}$$

and

$$\nu_L = \nu_T = \nu \tag{4}$$

where $c$ is the fiber volume fraction. Formula (2) is the rule of mixtures for the longitudinal stiffness, and (3) was given in [6] using the composite cylinders model. The remaining modulus, $E_T$, has a somewhat greater dependence on the spatial arrangement of the fibers. The approximation used here is taken from [6]

$$E_T = \frac{1+2\eta c}{1-\eta c}E_m \tag{5}$$

where

$$\eta = \frac{\dfrac{E_f}{E_m}-1}{\dfrac{E_f}{E_m}+2}. \tag{6}$$

The above formulas apply under the condition that no debonding occurs between the fiber and matrix in the plies. To obtain some insight into the role of fiber/matrix debonding, results will be computed in addition for the limiting case where it is assumed that the complete debonding has occurred. To model this, we have followed the suggestion in [5] and have taken $E_f = 0$ in (6), thereby reducing the transverse modulus. The effect of debonding on the longitudinal shear modulus is ignored since this effect is relatively unimportant.

Now consider a cross-ply laminate with equal thicknesses of 0 and 90° plies subject to in-plane

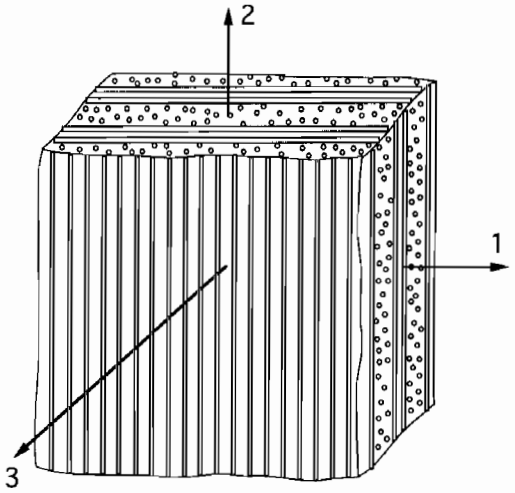


Fig. 2. Conventions for the 3D cross-ply laminate.

loading only, as illustrated in Fig. 2. A standard derivation based on the assumption that the in-plane strains are identical in every ply and that there are an equal number of 0 and 90° plies, gives the overall relation for the laminate to be

$$\epsilon_{11} = \frac{1}{E_0}\sigma_{11} - \frac{\nu_0}{E_0}\sigma_{22}$$

$$\epsilon_{22} = -\frac{\nu_0}{E_0}\sigma_{11} + \frac{1}{E_0}\sigma_{22}$$

$$\epsilon_{12} = \frac{1}{2\mu_0}\sigma_{12} \tag{7}$$

where

$$E_0 = \frac{\frac{1}{4}\left(1+\frac{E_L}{E_T}\right)^2 - \nu_L^2}{\frac{1}{2}\left(1+\frac{E_L}{E_T}\right)\left(\frac{1}{E_T}-\frac{\nu_L^2}{E_L}\right)}$$

$$\nu_0 = \frac{2\nu_L}{1+\frac{E_L}{E_T}}$$

$$\mu_0 = \mu_L \tag{8}$$

are Young's modulus, Poisson's ratio and shear modulus of the laminate, respectively, in the defined coordinates.

The plane strain Young's modulus defined as

$$\bar{E}_0 = \frac{E_0}{1-\nu_0^2} = \frac{\frac{1}{2}E_L\left(1+\frac{E_L}{E_T}\right)}{\frac{E_L}{E_T}-\nu_L^2} \tag{9}$$

will appear frequently in the sequel. Since the transverse modulus $E_T$ depends on whether the fiber/matrix interfaces are bonded or not, $\bar{E}_0$ also differs for these two cases.

### 2.2. *Concept of steady-state tunneling cracks*

Cracking in layered materials often occurs in the tunneling mode within individual layers, as illustrated in Fig. 1. The energy release rate at the tunnel front can be computed in principle by a three dimensional analysis. However, as the length of the tunnel becomes long compared with layer thickness, a steady-state is reached in which the same mode I energy release rate $G_{SS}$ is attained at every point on the front and is independent of tunnel length [7]. From an energy argument, the steady-state energy release rate $G_{SS}$ can be computed using quantities from the two-dimensional plane strain solution to the crack problem depicted in Fig. 3. The result is

$$G_{SS} = \frac{1}{2}\left\{\frac{1}{2t}\int_{-t}^{t}\sigma_0(x)\,\delta(x)\,dx\right\} \tag{10}$$

where $2t$ is the layer thickness, $\sigma_0$ is the stress normal to the crack surface prior to cracking, and $\delta$ is the crack opening displacement. This is applicable to linear elastic anisotropic materials and can be used when residual stress is present.

## 3. FINITE ELEMENT ANALYSIS

### 3.1. *Isolated cracks and the onset of tunnel cracking*

A complete analysis of the isolated crack problem depicted in Fig. 3, is performed by finite element analysis for all practical ranges of fiber volume fraction $c$ and the ratio of Young's modulus of fiber to matrix, for both bonded and separated fiber/matrix interfaces. The results for propagation of an isolated tunneling crack will be used to generate the conditions under which extensive matrix cracking first occurs.

Figure 3 shows the cross section of a laminate with a single transverse crack spanning the entire central 90° layer. The stress–strain behavior of each of the plies is taken to be elastically orthotropic obeying (1), with due regard for the two orientations. The interfaces between the layers are assumed to be perfectly bonded. Plane strain conditions are assumed in the $z$-direction and $\nu_m = \nu_f = 0.2$. The average tensile stress applied at infinity is $\sigma$, and the tensile stress in the 90° layer, prior to cracking, is

$$\frac{2E_T}{E_L+E_T}\sigma.$$

One can readily show that the normalized steady-state, tunneling energy release rate,

$$\frac{G_{SS}\bar{E}_0}{\sigma^2 t}$$

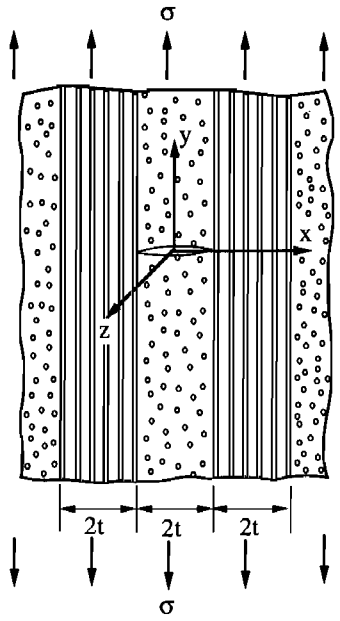


Fig. 3. An isolated crack in a 90° layer.

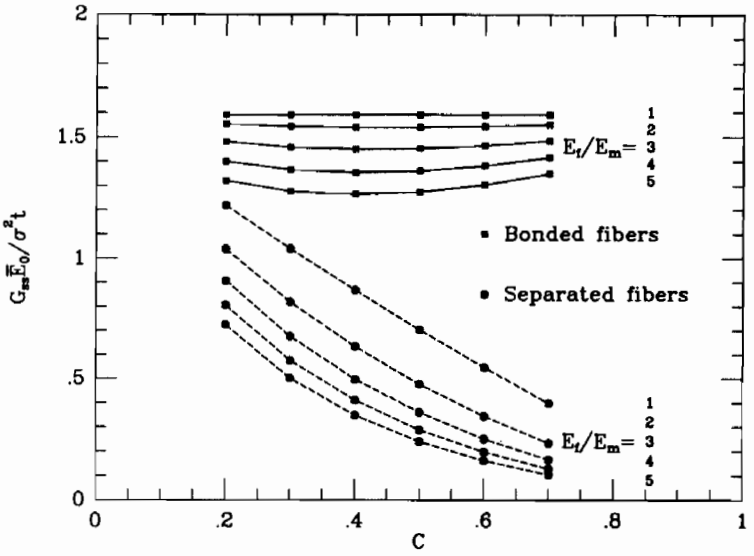


Fig. 4. The function, $f(E_f/E_m, c)$, providing the tunneling energy release rate in (11) for an isolated crack.

defined from (10) is a function only of fiber volume fraction $c$ and the modulus ratio $E_f/E_m$, assuming the Poisson's ratios have been assigned, i.e.

$$\frac{G_{SS}\bar{E}_0}{\sigma^2 t} = f\left(\frac{E_f}{E_m}, c\right) \tag{11}$$

where $\bar{E}_0$ is defined in (9) for the two cases, bonded and unbonded fibers mentioned in connection with (6). Results displaying the dependence are shown in Fig. 4 for the two cases. These results were computed using a 7-layer laminate model with the crack in the central layer, but they should apply for an arbitrary large number of layers with high accuracy. In fact, results computed using a 3-layer model and normalized in exactly the same way differ only very slightly from those shown in Fig. 4.

Denote the toughness of the layers in the tunneling cracking mode by $\Gamma$, measured in units of energy per unit area. For a crack propagating entirely in the matrix, this would be the mode I toughness of the matrix, $\Gamma_m$. For a tunnel crack front encompassing the unbonded interfaces between the fiber and matrix, $\Gamma$ would be some fraction of $\Gamma_m$. The minimum stress $\sigma_{onset}$ required for propagation of tunneling cracks in the 90° layers is obtained from (11) as

$$\sigma_{onset} = \sqrt{\frac{\Gamma\bar{E}_0}{tf\left(\frac{E_f}{E_m}, c\right)}}. \tag{12}$$

This sets the condition for the *onset* of extensive cracking in 90° layers. Note that this first cracking stress is inversely proportional to the square root of the ply thickness. If an initial residual tensile stress, $\sigma_R$, exists in the 90° layers acting parallel to the applied stress, then the sum of $\sigma_R(E_L + E_T)/(2E_T)$ and $\sigma_{onset}$ should appear on the left hand side of (12). In other words, residual tension in the layer, modified by the factor $(E_L + E_T)/(2E_T)$, is equivalent to an overall

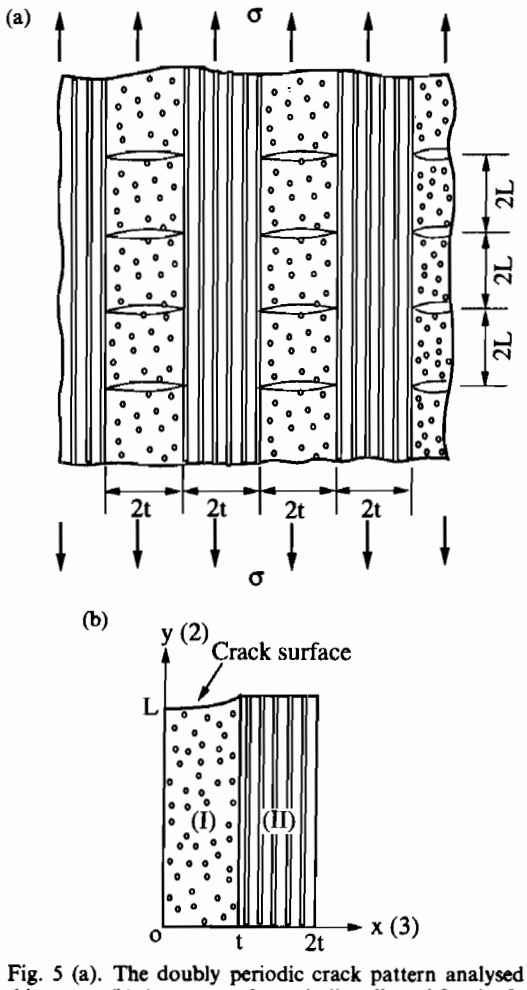


Fig. 5 (a). The doubly periodic crack pattern analysed in this paper. (b) A quarter of a periodic cell used for the finite element model.

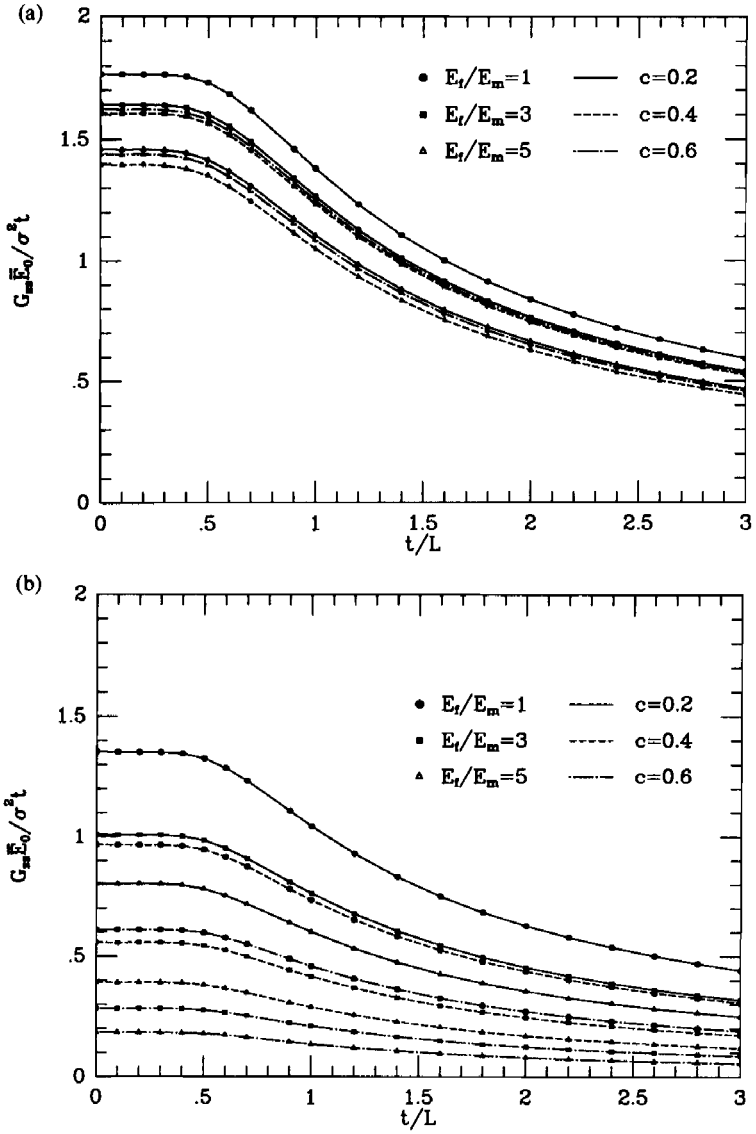


Fig. 6. The function, $g(E_f/E_m, c, t/L)$, providing the energy release rate for a doubly periodic array of tunneling cracks in (13). (a) Bonded fiber/matrix interfaces. (b) Separated fiber/matrix interfaces.

applied stress contribution as far as tunnel cracking is concerned.

### 3.2. *Multiple cracking*

Multiple cracking in 90° layers occurs when the applied stress exceeds the critical level given by (12). Results will be presented in this subsection for the doubly periodic, plane strain crack problem depicted in Fig. 5(a). Specifically, results will be presented which allow one to predict: (1) the evolution of crack density in the 90° layers, (2) the increase in overall compliance as a function of crack density, and (3) the extra overall strain released by the cracks in the presence of residual stress. The cracks are taken to be equally spaced within all 90° layers, with spacing $2L$ and with the doubly periodic pattern shown in Fig. 5(a). Plane strain conditions are again invoked and no traction is applied in the $x$-direction. Because of symmetry, only one quarter of a periodic cell needs to be considered in setting up the finite element model, which is shown in Fig. 5(b). Standard symmetry boundary conditions are applied on all edges of the quarter cell in Fig. 5(b) except along the crack face where traction-free conditions are imposed. The average traction on the vertical faces is required to vanish, consistent with the assumption that no stress is applied in the $x$-direction.

The finite element results for $G_{SS}$, expressed in non-dimensional form as

$$\frac{G_{SS}\bar{E}_0}{\sigma^2 t} = g\left(\frac{E_f}{E_m}, c, \frac{t}{L}\right) \tag{13}$$

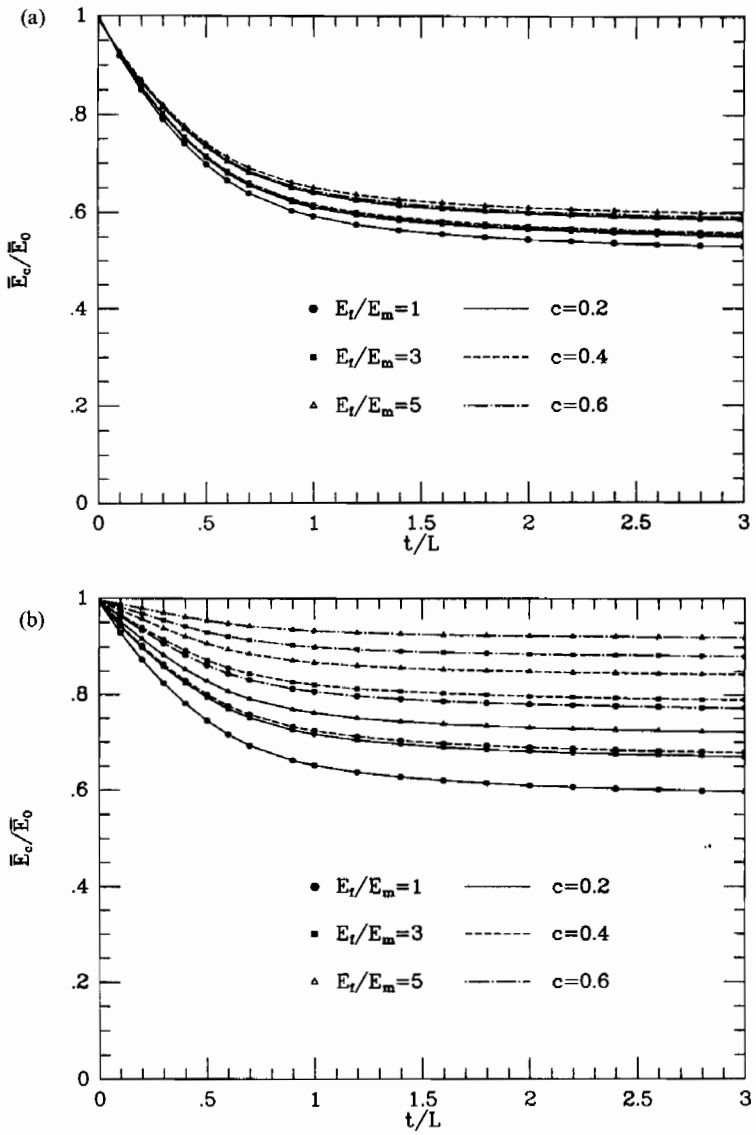


Fig. 7. The function, $h(E_f/E_m, c, t/L)$, providing the effective Young's modulus for the cracked laminate in (14). (a) Bonded fiber/matrix interfaces. (b) Separated fiber/matrix interfaces.

are shown in Figs 6(a,b), respectively, for bonded and separated fiber/matrix interfaces. In Section 4, it will be shown how to use this result for steady-state cracking to predict crack spacing as a function of applied stress. The corresponding results for the effective plane strain Young's modulus for the periodically cracked composite, defined as $\bar{E}_c = \sigma/\epsilon$ where $\epsilon$ is the average strain in the $y$ direction, are shown in Figs 7(a,b) as

$$\frac{\bar{E}_c}{\bar{E}_0} = h\left(\frac{E_f}{E_m}, c, \frac{t}{L}\right). \tag{14}$$

As the crack density $t/L$ becomes larger than about 2, the results have asymptoted to the limit in which only the 0° layers carry the load, which are simply

$$\frac{\bar{E}_c}{\bar{E}_0} = \frac{E_L}{E_L + E_T}. \tag{15}$$

It can be shown, by the reciprocal theorem of elasticity, that (13) and (14) are related by

$$\frac{1}{h\left(\frac{E_f}{E_m}, c, \frac{t}{L}\right)} = 1 + \frac{t}{2L} g\left(\frac{E_f}{E_m}, c, \frac{t}{L}\right). \tag{16}$$

Residual stresses and strains are generally introduced during the process when the plies are bonded together to form the layered composite. As discussed

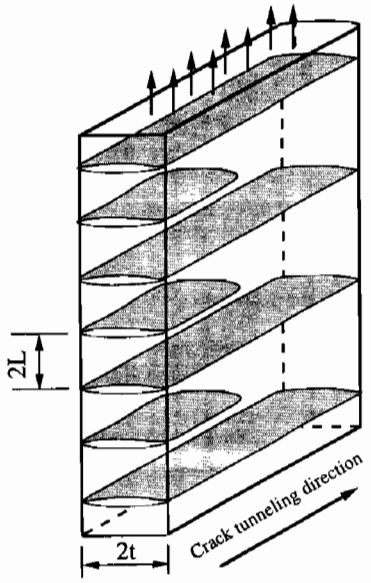


Fig. 8. A new set of tunneling cracks bisecting an existing set of cracks in a given layer.

earlier, if an initial, uniform residual stress $\sigma_R$ exists in the 90° layers acting parallel to the applied stress $\sigma$, the effect on the tunneling energy release rate is taken into account by replacing $\sigma$ on the left side of (13) by the sum of $\sigma_R(E_L + E_T)/(2E_T)$ and $\sigma$. An additional overall strain, $\epsilon_A$, occurs due to the release of residual stress by the formation of the cracks in the 90° layers. By a simple process of superposition (see Appendix), one can show that

$$\epsilon_A = \left(\frac{1}{\bar{E}_c} - \frac{1}{\bar{E}_0}\right)\frac{E_L + E_T}{2E_T}\sigma_R = (h^{-1} - 1)\frac{E_L + E_T}{2E_T}\frac{\sigma_R}{\bar{E}_0}. \tag{17}$$

In the limit where the crack spacing becomes small (i.e. $t/L$ becomes larger than about 2), the stress in the 0° layers due to the residual stress is reduced to zero. Consequently, in this limit, $\epsilon_A$ is just the negative of the initial strain in the 0° layers in the uncracked composite, i.e.

$$\epsilon_A = \frac{E_L + E_T}{2E_L}\frac{\sigma_R}{\bar{E}_0} = \left(1 - \frac{E_T}{E_L}\nu_L^2\right)\frac{\sigma_R}{E_L}. \tag{18}$$

## 4. APPLICATION TO PREDICT CRACK SPACING AND OVERALL STRESS–STRAIN BEHAVIOR

### *4.1. Prediction of crack spacing*

Results obtained in the last section will be used here to predict the tunneling crack spacing in 90° layers as a function of applied stress. The method employed here is identical to that of Hutchinson and Suo [7] used to predict the crack spacing in thin films under residual tension. It considers the effect of a sequential cracking process where a new set of cracks tunnels between an existing set of cracks as the stress is increased, rather than a process where all the cracks tunnel together.

The calculation of the energy release rate for the cracks tunneling in the sequential process makes use of the basic solution (13) for simultaneous steady-state cracking. That solution is for simultaneous tunneling of all the cracks, periodically spaced a distance $2L$ apart, in the 90° layers, as in Fig. 5. For any such laminate, the steady-state tunneling energy release rate for each crack is given by (13)

$$\frac{G_{SS}\bar{E}_0}{\sigma^2 t} = g\left(\frac{t}{L}\right) \tag{19}$$

where here the dependence of $g$ on $E_f/E_m$ and $c$ is left implicit. As noted before, when a residual stress $\sigma_R$

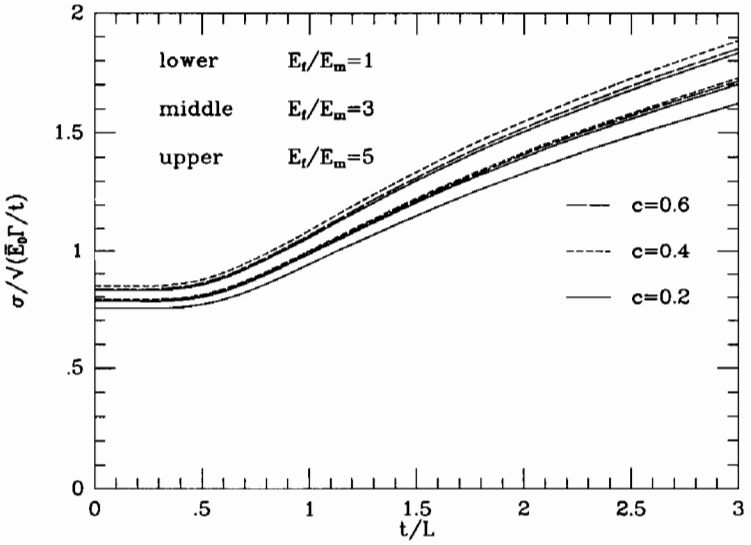


Fig. 9. Relationship between applied stress and crack spacing.

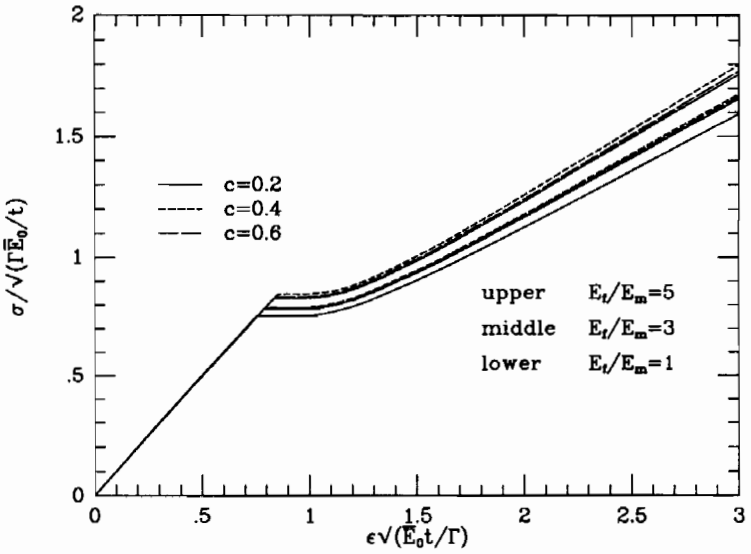


Fig. 10. Overall stress–strain behavior in the absence of residual stress.

exists in the 90° layers acting parallel to the overall applied stress $\sigma$, then $\sigma$ in the above formula should be replaced by $\sigma + (E_L + E_T)\sigma_R/(2E_T)$.

Now consider the sequential cracking situation depicted in Fig. 8, where one set of cracks spaced a distance $4L$ apart has already tunneled across all 90° layers, and where a second set bisecting the first set is in the process of tunneling across the layers. We depicted in Fig. 8 only an isolated 90° layer for better viewing. The steady-state energy release rate for the cracks in the process of tunneling can be obtained exactly from the strain energy difference far behind and far ahead of the tunneling fronts as

$$\frac{G_{SS}\bar{E}_0}{\sigma^2 t} = 2g\left(\frac{t}{L}\right) - g\left(\frac{t}{2L}\right). \tag{20}$$

Under the assumption that new cracks will always be nucleated half-way between cracks that have already formed and tunneled, and with $G_{SS}$ identified with the mode I toughness $\Gamma$ along fiber direction of 90° layers, (20) predicts the relationship between $\sigma$ and the crack spacing $t/L$. This relation is plotted in Fig. 9 for bonded fiber/matrix interfaces. There are two features worth noting. For spacing larger than $L/t$ of about 2, there is essentially no interaction between the cracks and the spacing is indeterminate by the present analysis. For smaller spacings the ratio $t/L$ increases approximately linearly with stress $\sigma$, and the dependence on the parameters $c$ and $E_f/E_m$ is largely captured in the non-dimensional stress variable $\sigma/\sqrt{(\bar{E}_0\Gamma/t)}$. Implicit in the spacing relationship in Fig. 9 is the assumption that initial flaws exist in the 90°

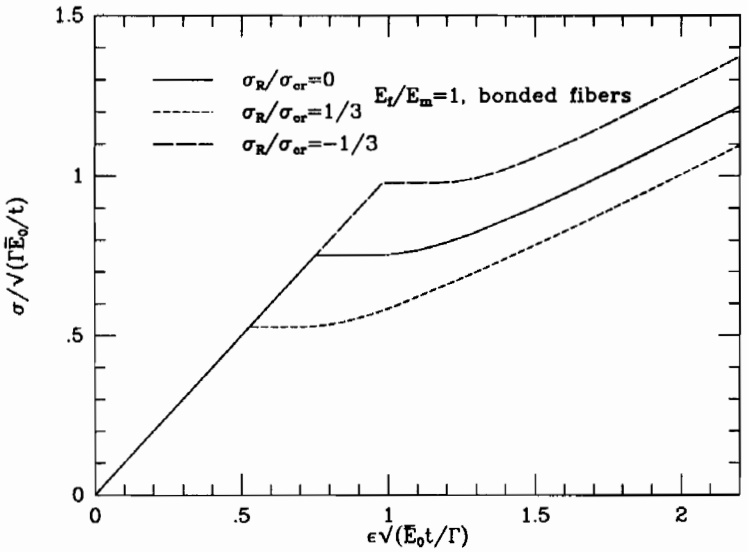


Fig. 11. An illustration of the effect of residual stress on overall stress–strain behavior.

layers of sufficient size and density such that the tunnel cracks *will* initiate when the steady-state condition is met. In this sense, the relation between spacing and stress may predict somewhat smaller spacings at a given stress than actually occurs.

### 4.2. *Prediction of overall stress–strain relation accounting for progressive cracking*

Let $\sigma$ be the overall stress applied to the composite and suppose that a residual stress $\sigma_R$ exists in the uncracked 90° layers acting parallel to the applied stress. With $\sigma$ replaced by $\sigma + (E_L + E_T)\sigma_R/(2E_T)$ in the non-dimensional stress variable on the ordinate in Fig. 9, the appropriate curve in this figure can be used to predict $t/L$ as a function of $\sigma$. Next, combine (14) and (17) to give the overall strain $\epsilon$ as

$$\epsilon = \frac{1}{\bar{E}_c}\sigma + \epsilon_A = \frac{1}{h}\frac{\sigma}{\bar{E}_0} + \left(\frac{1}{h} - 1\right)\frac{E_L + E_T}{2E_T}\frac{\sigma_R}{\bar{E}_0}. \quad (21)$$

Here $h(E_f/E_m, c, t/L)$ can be obtained from Fig. 7 once one has obtained the relation between $t/L$ and $\sigma$ as just described.

The calculations described above are now illustrated. In Fig. 10 plots are displayed of the normalized overall applied stress against the normalized overall strain for cases in which there is no residual stress. As noted earlier, the stress remains essentially unchanged until the crack spacing reaches an $L/t$ of about 2. This corresponds to the flat portion of the stress–strain curves in Fig. 10. As $L/t$ diminishes to small values (below about 1/2) the 0° layers carry most of the load, leading to the linear response evident in the figure, with (15) providing the asymptotic slope of these curves. A remarkable feature of these curves is the fact that the

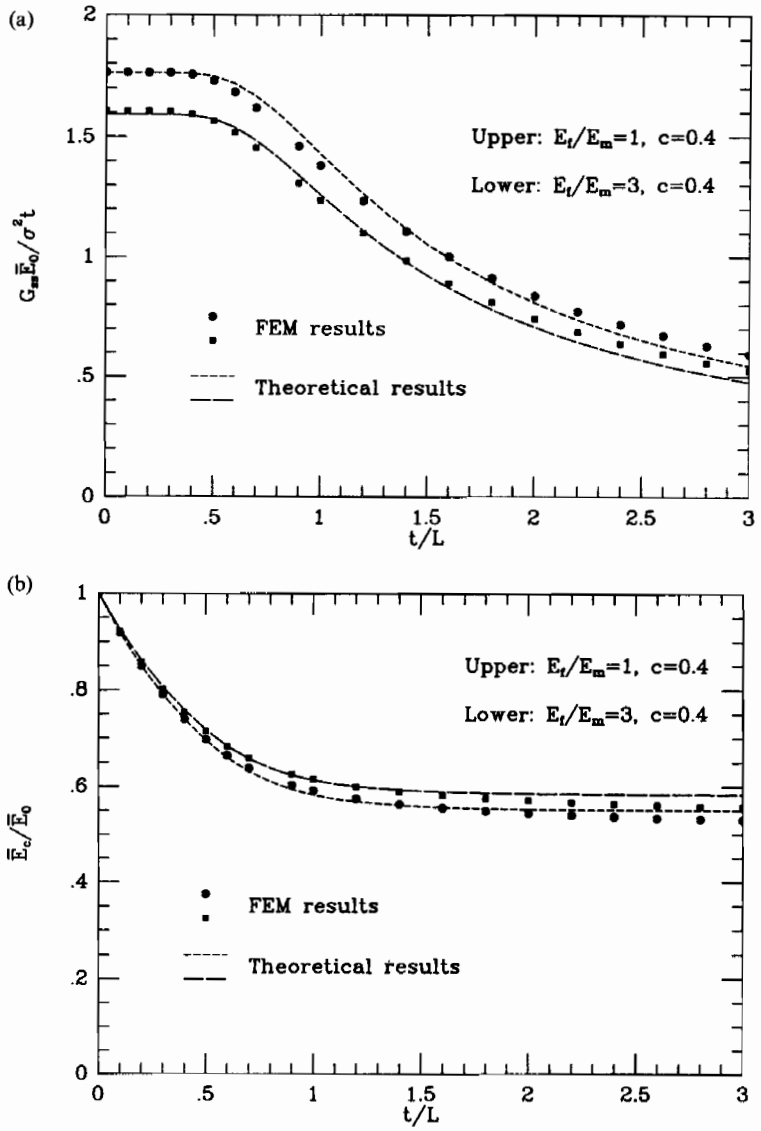


Fig. 12. (a) Demonstration of the accuracy of explicit formula (39). (b) Demonstration of the accuracy of explicit formula (41).

non-dimensional overall stress and strain variables used in Fig. 10 nearly collapse all the curves for a wide range of $E_f/E_m$ and $c$.

Figure 11 shows the effect of a residual stress $\sigma_R$ in the 90° layers, a positive value representing a residual tension and a negative value representing a residual compression. The critical stress $\sigma_{cr}$ used to normalize the residual stress in Fig. 11 is the stress at which cracks begin to tunnel in all the layers in the absence of any residual stress. From (13), this stress is

$$\sigma_{cr} = \sqrt{\frac{\bar{E}_0 \Gamma}{tg(E_f/E_m, c, 0)}}. \tag{22}$$

This critical stress is between 5 and 10% higher than the onset stress for tunneling of an isolated crack given by (12). In Fig. 11, $\sigma$ is the applied stress. Depending on its sign, the residual stress increases or decreases the applied stress at which matrix cracking occurs and makes a contribution to the overall strain due to its partial release.

## 5. AN APPROXIMATE THEORETICAL SOLUTION

### *5.1. The theoretical development*

In this section we shall develop an approximate analytical solution to the doubly periodic plane strain crack problem posed in Fig. 5(b). Except for a modification suggested at the end of this section, the approximation follows fairly closely a similar solution in [8], where it was developed to predict the stress transfer between 0 and 90° plies of a cracked laminate. The solution in [8] applies to periodic cracks in a single layer sandwiched between 0° layers on both sides. The following equilibrium equations must be satisfied in both 90° (denoted as material I) and 0° (denoted as material II) plies

$$\frac{\partial \sigma_x}{\partial x} + \frac{\partial \tau_{xy}}{\partial y} = 0 \tag{23}$$

$$\frac{\partial \tau_{xy}}{\partial x} + \frac{\partial \sigma_y}{\partial y} = 0. \tag{24}$$

The stress-strain relations for plane strain conditions can be easily derived from (1). They are, for 90° plies

$$\epsilon_x \equiv \frac{\partial u}{\partial x} = \left(\frac{1}{E_T} - \frac{\nu_L^2}{E_L}\right)\sigma_x - \left(\frac{\nu_T}{E_T} + \frac{\nu_L^2}{E_L}\right)\sigma_y \tag{25}$$

$$\epsilon_y \equiv \frac{\partial v}{\partial y} = -\left(\frac{\nu_T}{E_T} + \frac{\nu_L^2}{E_L}\right)\sigma_x + \left(\frac{1}{E_T} - \frac{\nu_L^2}{E_L}\right)\sigma_y \tag{26}$$

$$\epsilon_{xy} \equiv \frac{1}{2}\left(\frac{\partial u}{\partial y} + \frac{\partial v}{\partial x}\right) = \frac{1}{2\mu_T}\tau_{xy} \tag{27}$$

and for 0° plies

$$\epsilon_x \equiv \frac{\partial u}{\partial x} = \left(\frac{1-\nu_T^2}{E_T}\right)\sigma_x - \frac{\nu_L(1+\nu_T)}{E_L}\sigma_y \tag{28}$$

$$\epsilon_y \equiv \frac{\partial v}{\partial y} = -\frac{\nu_L(1+\nu_T)}{E_L}\sigma_x + \frac{1-\frac{E_T}{E_L}\nu_L^2}{E_L}\sigma_y \tag{29}$$

$$\epsilon_{xy} \equiv \frac{1}{2}\left(\frac{\partial u}{\partial y} + \frac{\partial v}{\partial x}\right) = \frac{1}{2\mu_L}\tau_{xy}. \tag{30}$$

The boundary conditions for a typical cell of the doubly periodic problem are the standard ones reflecting symmetry and the relations between the overall quantities and the averages of local quantities over the cell boundaries.

To proceed, we assume that the stress component $\sigma_y$ in both plies is independent of $x$. In other words, we look for an approximate solution of the form

$$\sigma_y^{I} = -F(y) + \sigma^{I} \tag{31}$$

$$\sigma_y^{II} = F(y) + \sigma^{II} \tag{32}$$

where $\sigma^{I}$ and $\sigma^{II}$ are the stresses in the 90 and 0° plies, respectively, that would result in a damage-free laminate subject to average remote tensile stress $\sigma$. They are given by

$$\sigma^{I} = \frac{2E_T}{E_T + E_L}\sigma \tag{33}$$

$$\sigma^{II} = \frac{2E_L}{E_T + E_L}\sigma. \tag{34}$$

We shall omit a detailed derivation for briefness; most of the details are similar to those given in [8]. After satisfying equations (23–25), (27), (28), (30) exactly, equations (26) and (29) in an average sense with respect to the $x$-direction, and satisfying all the boundary conditions except those listed below in (36) and (37), we obtain the following linear integral-differential equation for $F(y)$

$$t^4 F''''(y) - 2a_2 t^2 F''(y) + a_1^2 F(y) + a_0 \frac{1}{L}\int_0^L F(y)\,dy = 0 \tag{35}$$

where

$$a_2 = \frac{15}{2\Lambda}\left\{\left(\frac{1}{E_T} - \frac{\nu_L^2}{E_L} + \frac{1-\nu_T^2}{E_T}\right)\left(\frac{1}{\mu_T} + \frac{1}{\mu_L}\right) - 4\left[\left(\frac{1}{E_T} - \frac{\nu_L^2}{E_L}\right)\left(\frac{\nu_L(1+\nu_T)}{E_L}\right) + \left(\frac{\nu_T}{E_T} + \frac{\nu_L^2}{E_L}\right)\left(\frac{1-\nu_T^2}{E_T}\right)\right]\right\}$$

$$a_1^2 = \frac{45}{\Lambda}\left\{\left(\frac{1}{E_T} - \frac{\nu_L^2}{E_L} + \frac{1-\nu_T^2}{E_T}\right)\left(\frac{1}{E_T} - \frac{\nu_L^2}{E_L} + \frac{1-\frac{E_T}{E_L}\nu_L^2}{E_L}\right)\right.$$

$$-\left[\left(\frac{\nu_T}{E_T}+\frac{\nu_L^2}{E_L}\right)-\left(\frac{\nu_L(1+\nu_T)}{E_L}\right)\right]^2\Bigg\}$$

$$a_0=\frac{45}{\Lambda}\left[\left(\frac{\nu_T}{E_T}+\frac{\nu_L^2}{E_L}\right)-\left(\frac{\nu_L(1+\nu_T)}{E_L}\right)\right]^2$$

$$\Lambda=\left(\frac{1}{E_T}-\frac{\nu_L^2}{E_L}+\frac{1-\nu_T^2}{E_T}\right)^2+20\left(\frac{1}{E_T}-\frac{\nu_L^2}{E_L}\right)\left(\frac{1-\nu_T^2}{E_T}\right).$$

The remaining boundary conditions to be satisfied are given by

$$F(0)=0,\quad F(L)=\sigma^1,\quad \text{and}\quad F(L)=0. \tag{36}$$

In addition, it is required that $F(y)$ be an even function in $y$

$$F(y)=F(-y). \tag{37}$$

The solution to (35) can be used to express the integral of $F(y)$ as

$$\int_0^L F(y)\,dy=t\Phi\left(\frac{t}{L}\right)\sigma^1 \tag{38}$$

where $\Phi$ (which is also a function of $a_0$, $a_1$ and $a_2$) will be given below. The Young's modulus of the cracked composite, $\bar{E}_c$, is then approximately

$$\bar{E}_c\approx\frac{\sigma}{\bar{v}^{II}(L)/L}=\frac{\bar{E}_0}{1+\dfrac{t}{L}\dfrac{E_T}{E_L}\Phi} \tag{39}$$

and the tunneling energy release rate $G_{SS}$, calculated from

$$G_{SS}=\sigma^1[\bar{v}^{II}(L)-\bar{v}^{I}(L)] \tag{40}$$

is given by the approximation

$$\frac{G_{SS}\bar{E}_0}{\sigma^2 t}=\frac{2E_T}{E_L}\Phi \tag{41}$$

In equations (39) and (40), terms such as $\bar{v}(L)$ stand for the average $y$-displacement along $y=L$.

For the case $a_2/a_1$ is less than 1, $\Phi$ is given by

where

$$m=\sqrt{(a_1+a_2)/2}$$
$$n=\sqrt{|a_1-a_2|/2}$$
$$h=\frac{a_0}{a_0+a_1^2}.$$

For cases where $a_2/a_1$ is equal to or greater than 1, similar solutions can be obtained. However, for most practical fiber-reinforced composites, $a_2/a_1$ is either less than 1 or sufficiently close to 1 such that (42) is a good approximation.

### 5.2. *Modification using the FEM results*

The analytical approximation given by equations (39), (41) and (42) can be further enhanced by a slight modification of $\Phi$ in (42), which was suggested by the comparison of the approximate predictions with the more accurate FEM results obtained in Section 3. We found that the accuracy of the above approximation was improved when we replaced $m$ and $n$ is (42) by $1.1m$ and $1.1n$, respectively, and then multiplied $\Phi$ by the numerical factor of 0.82. Thus the modified $\Phi$ is given by

$$\Phi\left(\frac{t}{L}\right)=\frac{0.82\dfrac{2(1-h)mn}{m^2+n^2}\left(\cosh\dfrac{2.2mL}{t}-\cos\dfrac{2.2nL}{t}\right)}{1.1m\sin\dfrac{2.2nL}{t}+1.1n\sinh\dfrac{2.2mL}{t}-\dfrac{2hmn}{m^2+n^2}\dfrac{t}{L}\left(\cosh\dfrac{2.2mL}{t}-\cos\dfrac{2.2nL}{t}\right)}. \tag{43}$$

Several comparisons of the results given by FEM analysis and the explicit formulas of equations (39) and (41) are demonstrated in Figs 12(a,b). The differences for all practical ranges of $E_f/E_m$ and $c$ are within 5%, and thus we believe the formulas given above are well suited for practical applications.

*Acknowledgements*—This work was supported in part by the DARPA URI (Subagreement P.O. # KK3007 with the University of California, Santa Barbara, ONR Prime Contract N00014-92-J-1808) and by the Division of Applied Sciences, Harvard University. Finite element analyses are carried using ABAQUS (Hibbitt, Karlsson & Sorensen Inc., Providence, Rhode Island, U.S.A.).

## REFERENCES

1. D. H. Allen, C. E. Harris and S. E. Groves, *Int. J. Solids Struct.* **23**, 1301 (1987).
2. D. H. Allen, C. E. Harris and S. E. Groves, *Int. J. Solids Struct.* **23**, 1319 (1987).
3. P. Gudmundson and S. Ostlund, *J. Comp. Mater.* **26**, 1009 (1992).

$$\Phi\left(\frac{t}{L}\right)=\frac{\dfrac{2(1-h)mn}{m^2+n^2}\left(\cosh\dfrac{2mL}{t}-\cos\dfrac{2nL}{t}\right)}{m\sin\dfrac{2nL}{t}+n\sinh\dfrac{2mL}{t}-\dfrac{2hmn}{m^2+n^2}\dfrac{t}{L}\left(\cosh\dfrac{2mL}{t}-\cos\dfrac{2nL}{t}\right)} \tag{42}$$

4. P. Gudmundson and W. Zang, SICOMP Tech. Report 92-007 (1992).
5. D. S. Beyerle, S. M. Spearing and A. G. Evans. *J. Am. Ceram. Soc.* **75,** 3321 (1992).
6. R. M. Christensen, *Mechanics of Composite Materials.* Wiley, New York (1979).
7. J. W. Hutchinson and Z. Suo, in *Advances in Applied Mechanics* (edited by J. W. Hutchinson and T. Y. Wu), Vol. 29, p. 64. Academic Press, New York (1991).
8. L. N. McCartney, *J. Mech. Phys. Solids* **40,** 27 (1992).

## APPENDIX

When an initial residual stress $\sigma_R$ exists in the 90° layers acting parallel to the applied stress, an additional overall strain $\epsilon_A$ occurs due to the release of residual stress by the formation of the cracks in the 90° layers. This additional strain can be calculated by applying a normal stress of $(-\sigma_R)$ to the crack surface. Figure A1(a) depicts a quarter of such a periodic cell, with standard symmetry boundary conditions applied. By a linear superposition argument, one can easily verify that the displacement and stress fields of Fig. A1(a) can be obtained by subtracting that in Fig. A1(c) from Fig. A1(b), where (b) has the same crack configuration as (a), and (c) depicts the crack-free laminate. The elements in (b) and (c) are both subject to an average stress $(E_L + E_T)\sigma_R/(2E_T)$. The overall strain $\epsilon_b$ associated with (b) is given by (14)

$$\epsilon_b = \frac{1}{E_c}\frac{E_L + E_T}{2E_T}\sigma_R = h^{-1}\frac{E_L + E_T}{2E_T}\frac{\sigma_R}{E_0} \tag{A1}$$

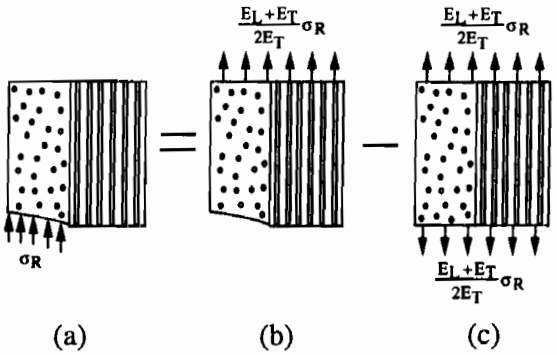


Fig. A1. Superposition for obtaining $\epsilon_A$ due to the release of residual stress.

and the overall strain $\epsilon_c$ in (c) is given by a uniform plane strain tension

$$\epsilon_c = \frac{1}{E_0}\frac{E_L + E_T}{2E_T}\sigma_R. \tag{A2}$$

The overall strain $\epsilon_A$ in (a) is then

$$\epsilon_A = \epsilon_b - \epsilon_c = (h^{-1} - 1)\frac{E_L + E_T}{2E_T}\frac{\sigma_R}{E_0} \tag{A3}$$

which is (16) given in Section 3.